ASM Sc. J., 13, Special Issue 2, 2020 for ICSCC2019, 46-55

Modelling of Maximum Power Point Tracking based Controller for Grid Tie Quasi Z Source Inverter

Law Kah Haw

Department of Electrical and Computer Engineering, Curtin University, Miri, Malaysia

Quasi Z source inverter (qZSI) has been preferable to perform DC-AC buck/boost inversion when compared with traditional two-stage topology due to its single stage configuration. This work extended the analysis and investigation of qZSI for photovoltaic (PV) system. The DC-link voltage of qZSI is regulated via the proposed dual-loop controller to ensure constant voltage level in regardless of changing of loading conditions as well as varying of solar irradiance and temperature. On the other hand, maximum power point tracking (MPPT) scheme is utilized in conjuction with carrier based pulse width modulation (CB-PWM) technique to ensure maximum power extraction from the PV array. All aforementioned outcomes are theoretically validated in simulation with mathematics. The proposed qZSI is then employed to grid as static synchronous compensator (STATCOM) for enhancing power factor.

Keywords: Quasi Z Source Inverter (qZSI); Photovoltaic (PV) system; maximum power point tracking (MPPT)

I. INTRODUCTION

Renewable energy is high in demand nowadays due to the change in environmental conditions globally. As the majority of power generation at the present time depends on fossil fuel, the power plant may possess hazard which harm the environment. By using renewable energy resources (RERs) as an alternative source for power generation, the emission of greenhouse gases (GHG) can be reduced, simultaneously, customers and utilities can also be benefited economically (Rehmani *et al.* 2018). There are different kinds of RERs available such as solar, hydro and wind energy. Solar energy is considered a great source of renewable energy because of its high availability and does not bring any negative impacts to the environment. The PV system is categorized into three classifications, mainly the standalone mode, hybrid and grid-tie PV systems. The standalone PV system is the best option to date and it is also suitable to be implemented in rural area due to its reliability and clarity. As the consistency of solar energy varies throughout the day, hence the efficiency of the PV array will not be ideal. The current and voltage produced by the PV array is affected by the solar irradiance and temperature, respectively, and this will also affect the efficiency of the PV array. To overcome this problem, MPPT is required to track the maximum power. Different kinds of MPPT algorithm have been implemented such as P&O, Incremental Conductance (IncCond) and fuzzy logic control. These algorithms vary from each other in terms of implementation complexity, speed of convergence and sensed parameters (Gorgani *et al.* 2016; Chung *et al.* 2016; Hanaah *et al.* 2017, Law *et al.* 2019a; 2019b, Cindy *et al.* 2019).

To ensure that an ideal amount of maximum power can be delivered from the PV array to the load, a DC-DC converter is required to be placed between the array and the load. In a nutshell, a PV system consists of PV array, DC-DC converter and DC-AC inverter. Normally, buck, boost, and buck-boost converters are widely used for PV implementation but they are only restricted to low power applications (Law *et al.* 2011; 2012; 2014a; 2014b; 2017; 2019c; Meraj *et al.* 2019a; 2019b). The use of conventional converters can be replaced by qZSI as it has several unique features such as lower voltage stress,

*Corresponding author's e-mail: lawkahhaw@curtin.edu.my

constant DC current from the PV array, twice the output power versus the input one, and can operate with no dead-band, which makes it more favourable to be implemented in a PV system (Ong *et al.* 2018; Law *et al.* 2019d; 2019e; 2019f; Sia *et al.* 2019). The circuit topology of the qZSI was introduced in 2008 and it is the improved version of the Z-Source Inverter (ZSI). The improvements include less switching pulse, continuous DC current from the source and the minimization of voltage stress on the capacitor. Besides, the qZSI also has the ability to perform voltage buck/boost functions in a single stage. These characteristics outshine the performance of a conventional voltage source inverter (VSI) where an additional DC-DC converter is needed to step-up or step-down the DC voltage in order to obtain the suitable DC-link voltage and then inverted into AC form afterwards. With this quality of the qZSI, it is highly applicable for applications which use renewable energy as the main source.

This paper focused on developing two controllers for the qZSI; namely the grid-tie controller and the dual-loop DC-link voltage controller. The first controller ensures maximum power to be extracted and delivered to the load whereas the latter controller ensures constant DC-link voltage under different solar irradiance and temperature. Furthermore, unipolar CB-PWM technique is employed in this work to attain the single-phase AC output voltage waveform. This paper is arranged in the following order: Section II explains the operation of the qZSI and the P&O MPPT algorithm. Section III reveals the design implementation of the proposed controllers. Simulation results are analyzed, discussed and presented in Section IV. Lastly, conclusions are made in Section V.

II. OPERATING PRINCIPLES OF QZSI AND MPPT ALGORITHM

A. Quasi Z Source Inverter

Figure 1 depicts the schematic of qZSI. The operation of qZSI consists of two operating states known as the shoot-through state and non-shoot-through state (i.e., active state) detailed in (Ong *et al.* 2018). During the shoot-through state, all switches (i.e., Q_1, Q_2, Q_3, and Q_4) can be gated on simultaneously forcing the diode to be off.

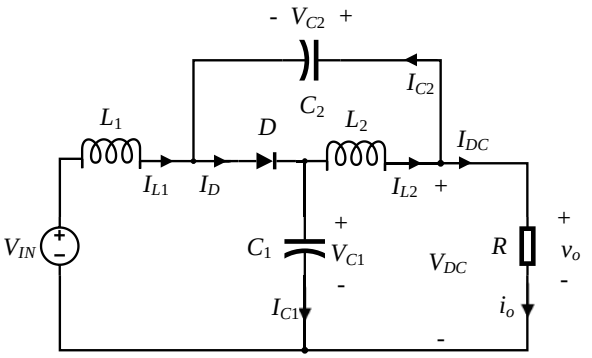

Figure 1. Quasi Z source inverter

During the active state, switches Q_1 and Q_4 or Q_2 and Q_3 are gated on sequentially and the diode is in forward biased; charging up all the capacitors via the DC input voltage and the energy discharged from the inductors. The state-space equations of qZSI which govern the shoot-through state D_O and active state $1\text{-}D_O$ can be found in (Sia *et al.* 2019) where its passive components are represented by inductors L_1 and L_2, capacitors C_1 and C_2; current flowing through both inductors is represented by I_{L1} and I_{L2}; voltage across both capacitors is V_{C1} and V_{C2}; DC input voltage is V_{IN}; DC output current is I_{DC}, and the steady-state shoot-through duty ratio is represented by D_O. The operating time period of the qZSI over one switching cycle is given by:

$$T_S = D_O + (1 - D_O) = 1 \tag{1}$$

where T_S is also the inverse of switching frequency f_{SW}.

The relationship governed by I_{L1}, I_{L2}, V_{C1}, V_{IN}, I_{DC}, and V_{DC} are derived in (2)-(9).

$$I_{L1} = I_{L2} \tag{2}$$

$$I_{DC} = I_{L1} + I_{L2} \tag{3}$$

$$V_{IN} = V_{C1} - V_{C2} \tag{4}$$

$$V_{DC} = V_{C1} + V_{C2} \tag{5}$$

$$\overline{V_{DC}} = V_{C1} \tag{6}$$

$$\frac{V_{C1}}{V_{IN}} = \frac{1 - D_O}{1 - 2D_O} \tag{7}$$

$$\frac{V_{C2}}{V_{IN}} = \frac{D_O}{1 - 2D_O} \tag{8}$$

$$\frac{V_{DC}}{V_{IN}} = \frac{1}{1 - 2D_O} = \beta \tag{9}$$

where β in (9) represents the boost factor of qZSI.

It can be understood that the value of shoot-through duty ratio D_O cannot be equal to or more than 0.5 as to prevent the DC-link voltage from reaching infinity.

B. MPPT Algorithm

Climate change such as the weather variation leads to inconstancy of solar energy absorbed by the PV array. Therefore, the employment of MPPT is necessitate to improve its power extraction efficiency. In this paper, the P&O MPPT algorithm is utilized due to its less complexity in implementation. With P&O method, the perturbation of the PV voltage is involved based on the comparison made between the present power measured from the PV array and the perturbation of power stored in the memory. After it has come to the realization that the present power is larger than the perturbation power in the memory, the algorithm will compare the previous PV voltage with the present PV voltage in order to identify its maximum power point via the determined direction of perturbation. Figure 2 shows the concept of P&O MPPT algorithm.

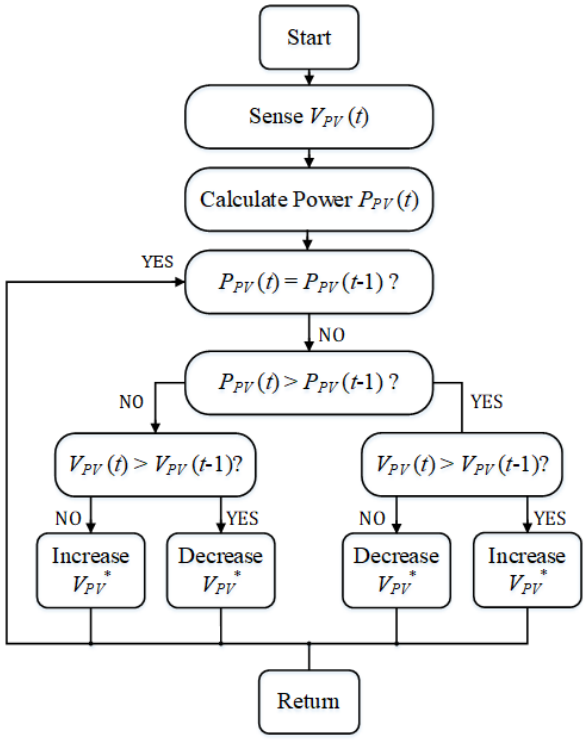

Figure 2. Working principle of P&O MPPT algorithm

III. QZSI AND CONTROL SCHEME MODELLING

Figure 3 illustrates the simulation model of qZSI controlled via the proposed grid-tie and dual-loop DC-link controllers.

A. Grid-tie controller

The grid-tie controller is structured with one outer voltage loop and an inner current loop to ensure similar input and output power profile. In other words, this controller outputs the desired magnitude of modulating waveform for the CB-PWM technique according to the weather condition.

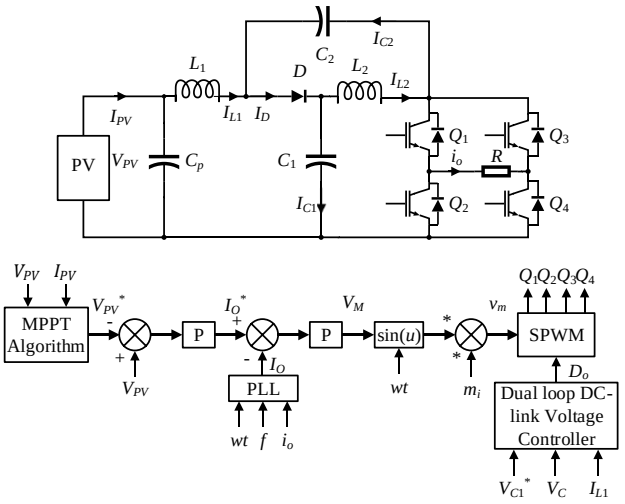

Figure 3. Proposed PV integrated qZSI model

Figure 4 depicts the simulation model of the proposed grid-tie controller. From Figure 4, both P controllers are tuned via the Simulink control design PID tuning tools while C_p is the smoothing capacitor connected in parallel with the PV array.

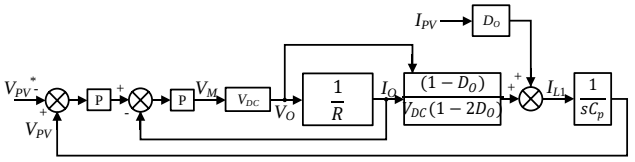

Figure 4. Proposed grid-tie controller

At active state, the qZSI acts as a traditional H-bridge inverter where the non-shoot-through DC-link voltage is given by:

$$V_{DC,nsh} = \frac{1}{1-2D_O} V_{PV} = V_{DC} \quad (10)$$

At shoot-through state, no voltage is supplied by the qZSI and thus:

$$V_{DC,sh} = 0 \tag{11}$$

The output power is twice than the input power at active state as derived below:

$$2V_{PV}I_{L1.nsh} = I_O V_O \tag{12}$$

From (10) and (12), the current flows through inductor L_1 at active state is formed as follows:

$$I_{L1,nsh} = \frac{I_O V_O}{2V_{PV}} = \frac{I_O V_O}{2V_{DC}(1-2D_O)} \tag{13}$$

Subsequently, at shoot-through state, the inductor current I_{L1} is given by:

$$I_{L1,sh} = I_{PV} \tag{14}$$

where I_{PV} is the current produced by the PV array.

The aforementioned equations yield the inductor current I_{L1} to flow through inductor L_1 over one switching cycle as derived below:

$$I_{L1} = I_{PV}D_O + \frac{I_O V_O(1-D_O)}{2V_{DC}(1-2D_O)} \tag{15}$$

By using KVL, the following equation can be obtained from the qZSI model:

$$V_O = I_O R \tag{16}$$

where V_O is the peak value of qZSI AC output voltage and R represents the resistive load.

B. Dual-loop DC-link Voltage controller

The dual-loop DC-link voltage controller is proposed to generate the desired shoot-through duty ratio that ensures constant DC-link voltage under varying solar irradiance and temperature. In contrast to traditional controllers, the proposed dual-loop controller is able to cancel out disturbances, achieve faster dynamic and transient performances as well as stabilize the voltage across the DC-link of qZSI.

Through small-signal analysis, the state-space equations of qZSI which govern the shoot-through state and active state are derived in (17) and (18), respectively, by taking the inductors' stray resistances (i.e., r_L=r_{L1}=r_{L2}) and capacitors' series resistances (i.e., r_C=r_{C1}=r_{C2}) into consideration.

$$\begin{bmatrix} \dot{I}_{L1} \\ \dot{I}_{L2} \\ \dot{V}_{C1} \\ \dot{V}_{C2} \end{bmatrix} = \begin{bmatrix} -\frac{r_L + r_C}{L} & 0 & 0 & \frac{1}{L} \\ 0 & -\frac{r_L + r_C}{L} & \frac{1}{L} & 0 \\ 0 & -\frac{1}{C} & 0 & 0 \\ -\frac{1}{C} & 0 & 0 & 0 \end{bmatrix} \begin{bmatrix} I_{L1} \\ I_{L2} \\ V_{C1} \\ V_{C2} \end{bmatrix} + \begin{bmatrix} \frac{1}{L} & 0 \\ 0 & 0 \\ 0 & 0 \\ 0 & 0 \end{bmatrix} \begin{bmatrix} V_{IN} \\ I_{DC} \end{bmatrix} \tag{17}$$

$$\begin{bmatrix} \dot{I}_{L1} \\ \dot{I}_{L2} \\ \dot{V}_{C1} \\ \dot{V}_{C2} \end{bmatrix} = \begin{bmatrix} -\frac{r_L + r_C}{L} & 0 & -\frac{1}{L} & 0 \\ 0 & -\frac{r_L + r_C}{L} & 0 & -\frac{1}{L} \\ \frac{1}{C} & 0 & 0 & 0 \\ 0 & \frac{1}{C} & 0 & 0 \end{bmatrix} \begin{bmatrix} I_{L1} \\ I_{L2} \\ V_{C1} \\ V_{C2} \end{bmatrix} + \begin{bmatrix} \frac{1}{L} & \frac{r_C}{L} \\ 0 & \frac{r_C}{L} \\ 0 & -\frac{1}{C} \\ 0 & -\frac{1}{C} \end{bmatrix} \begin{bmatrix} V_{IN} \\ I_{DC} \end{bmatrix} \tag{18}$$

By equating (17) and (18), the non-linear time-invariant state-space averaging equation over one switching cycle is represented in first-order differential forms as given in (19).

$$\begin{bmatrix} \dot{I}_{L1} \\ \dot{I}_{L2} \\ \dot{V}_{C1} \\ \dot{V}_{C2} \end{bmatrix} = \begin{bmatrix} -\frac{r_L + r_C}{L} & 0 & -\frac{1-D_O}{L} & \frac{D_O}{L} \\ 0 & -\frac{r_L + r_C}{L} & \frac{D_O}{L} & -\frac{1-D_O}{L} \\ \frac{1-D_O}{C} & -\frac{D_O}{C} & 0 & 0 \\ -\frac{D_O}{C} & \frac{1-D_O}{C} & 0 & 0 \end{bmatrix} \begin{bmatrix} I_{L1} \\ I_{L2} \\ V_{C1} \\ V_{C2} \end{bmatrix} + \begin{bmatrix} \frac{1}{L} & \frac{r_C(1-D_O)}{L} \\ 0 & \frac{r_C(1-D_O)}{L} \\ 0 & -\frac{1-D_O}{C} \\ 0 & -\frac{1-D_O}{C} \end{bmatrix} \begin{bmatrix} V_{IN} \\ I_{DC} \end{bmatrix} \tag{19}$$

Due to akin state vectors from (19), the final essential transfer functions of qZSI needed in this work are derived in (20) (i.e., qZSI current transfer function G_{iL}) and (21) (i.e., qZSI voltage transfer function G_{vC}) after taking laplace transform and considering the perturbation behavior of state variables to (19):

$$\frac{\tilde{\imath}_L(s)}{\tilde{d}_o(s)} = \frac{sC(v_{c1} + v_{c2} - i_{dc}r_C) + (1-2d_o)(i_{dc} - i_{L1} - i_{L2})}{s^2LC + sC(r_L + r_C) + (1-2d_o)^2} \tag{20}$$

$$\frac{\tilde{v}_c(s)}{\tilde{d}_o(s)} = \frac{(sL + (r_L + r_C))(i_{dc} - i_{L1} - i_{L2}) + (1 - 2d_o)(v_{c1} + v_{c2} - i_{dc}r_C)}{s^2LC + sC(r_L + r_C) + (1 - 2d_o)^2} \quad (21)$$

Figure 5 depicts the single-line diagram of the proposed dual-loop DC-link voltage controller.

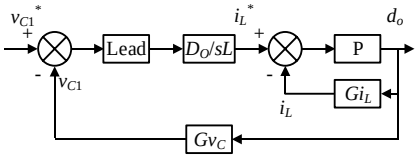

Figure 5. Proposed dual-loop DC-link voltage controller

Its P controller is tuned via the Simulink control design PID tuning tools. The details of the transfer function of lead compensator and the novel technique to find its parameters can be found in (Yong *et al.* 2018).

IV. SIMULATION RESULTS AND DISCUSSION

The proposed controllers and the P&O MPPT algorithm are integrated into the qZSI model to verify its effectiveness via MATLAB/Simulink. The proposed qZSI model is simulated under three conditions: using 1) a DC voltage source as the input source without MPPT, 2) PV array as the input source with MPPT at constant solar irradiance and temperature, 3) PV array as input source with MPPT and varying solar irradiance and temperature. All simulation parameters are as listed in Table 1 below:

Table 1. System parameters used in QZSI for simulation purposes

Parameters	**Value**
Input Voltage, V_{IN}	24 V
Capacitor voltage reference, v_{c1}^*	48 V
Switching frequency, f_{SW}	100 kHz
Steady-state shoot-through duty ratio, D_O	0.33
Inductance, L_1=L_2	100 μH
Capacitance, C_1=C_2	1000 μF
Internal inductor resistance, r_{L1}= r_{L2}	32.2 mΩ
Internal capacitor resistance, r_{C1}= r_{C2}	56 mΩ
Load resistor, R	26 Ω
Smoothing capacitance, C_p	50 nF

A. QZSI with DC input voltage source

The proposed qZSI model was simulated with a 24 V battery as the DC input voltage source. Under the same loading condition, the modulation index m_i was purposely step changes from 0.67 to 1.34 at 0.5 s to validate the effectiveness of the dual-loop DC-link voltage controller. Specifically, Figure 6(a) depicts that the resultant shoot-through duty ratio d_o was constant throughout the 1 s of simulation period under different value of modulation index m_i (see Figure 6(d)). This reflects to achieve constant voltage amplitude measured across capacitor C_1 (see Figure 6(b) and Figure 6(c)) which consistently tracked the capacitor reference voltage v_{c1}^*. Moreover, with (4), the DC input voltage level connected to the qZSI can determined from Figure 6(c).

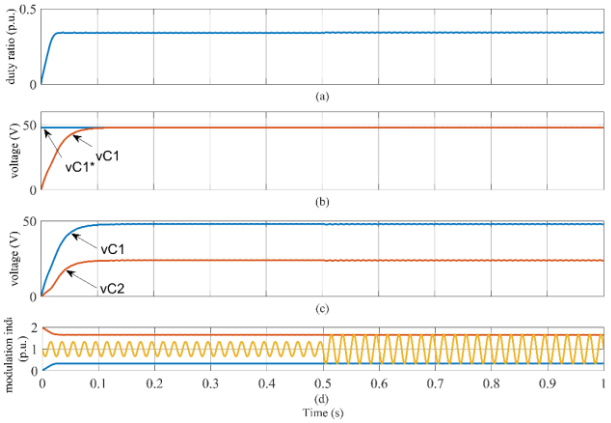

Figure 6. Simulation results of the proposed single-phase qZSI model with battery as input voltage source (a) shoot-through duty ratio d_o, (b) reference v_{C1}^* and measured v_{C1} voltages across capacitor C_1, (c) voltages measured across capacitor C_1 and C_2, and (d) modulating waveform v_m.

B. QZSI with PV array under constant solar irradiance and temperature

The feasibility of the proposed qZSI model was then justified through simulation with the PV array employed as the DC input voltage source under constant solar irradiance and temperature. With the same simulation period of 1 s, the proposed model was simulated according to the meteorological analysis in Malaysia, with an average solar irradiance and temperature of 1470 kW/m² and 25°C,

respectively, as depicted in Figure 7 below:

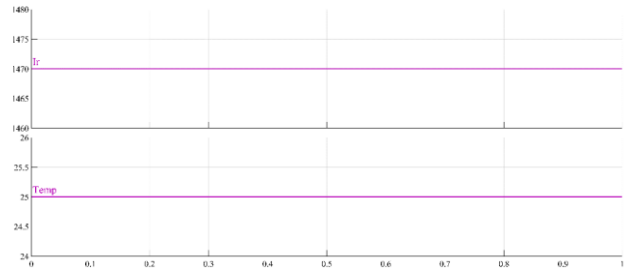

Figure 7. Constant of solar irradiance (top) and temperature (bottom)

Figure 8(a) depicts the practicability of the dual-loop DC-link voltage controller which was, once again, able for the voltage across capacitor C_1 to track its reference voltage v_{c1}^* value (see Figure 8(b)).

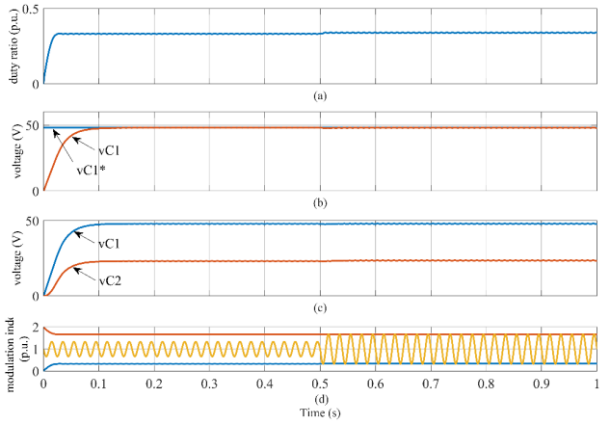

Figure 8. Simulation results of the proposed single-phase qZSI model with PV array as input voltage source under constant solar irradiance and temperature (a) shoot-through duty ratio d_o, (b) reference v_{C1}^* and measured v_{C1} voltages across capacitor C_1, (c) voltages measured across capacitor C_1 and C_2, and (d) modulating waveform v_m

C. QZSI with PV array under varying solar irradiance and temperature

In this section, the simulation was carried out by varying the solar irradiance and temperature to further validate the workability of the proposed qZSI model. The simulation period was set at 6 s starting with the initial solar irradiance and temperature values of 1470 W/m² and 25 °C, respectively. The aforementioned parameters values were then deviated according as illustrated in Figure 9 below:

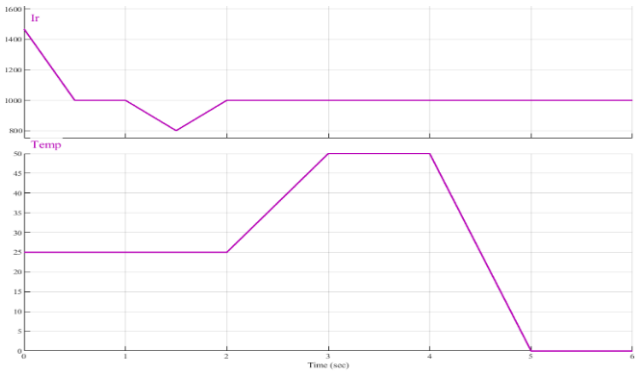

Figure 9. Variation of solar irradiance (top) and temperature (bottom)

The fluctuation of the solar irradiance and temperature simulates the real-life condition of the inconsistent energy that the PV array received. By referring to (Islam *et al.* 2014; Skoplaki & Palyvos 2009), the changes of solar irradiance will affect the PV array's current output whereas the changes of temperature will influence the voltage produce across the PV array. From Figure 9, it is observed that there were ramp changes of solar irradiance from 1470 W/m² to 1000 W/m² at 0.5 s followed by 800 W/m² to 1000 W/m² at 2 s. During this period, the solar temperature was remained constant at 25 °C indicating that the voltage V_{PV} produced by the PV array was constant while the PV current I_{PV} was varied. From simulation time of 2 s, the temperature has risen up from 25 °C to 50 °C which, theoretically, causing the PV array voltage V_{PV} to drop. In contrast, the PV array voltage V_{PV} should increase from 4 s onwards as the temperature were reduced from 50 °C to 0 °C.

The conclusion drawn from the previous paragraph states that, without any controller, the inductor currents (i.e., i_{L1} and i_{L2}) would varied from 0 s to 2 s (see Figure 10) while the average of the qZSI DC-link voltage V_{DC} or the capacitor voltage v_{C1} supposedly would varied from 2 s and onwards.

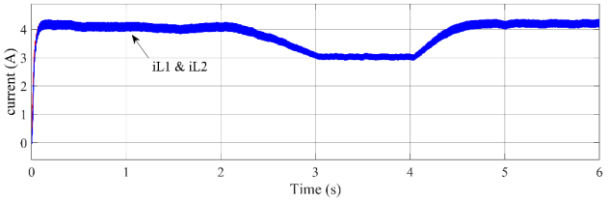

Figure 10. Simulation results of inductor currents i_{L1} and i_{L2}

Nevertheless, with the integration of the proposed dual-loop DC-link voltage controller, the aforementioned voltage

parameters remained constant throughout the 6 s of simulation time (see Figure 11(b) and Figure 11(c)) despite the variation in the irradiance and temperature.

Furthermore, with the proposed grid-tie controller and P&O MPPT algorithm, the profile of both the DC input power P_{PV} and DC output power P_{DC} characteristics were identical despite the variation in the solar irradiance and temperature as shown in Figure 12.

Figure 13 depicted both the DC-link voltage V_{DC} and current I_{DC} measured from the qZS network demonstrating transient stability performance offered by the proposed controllers.

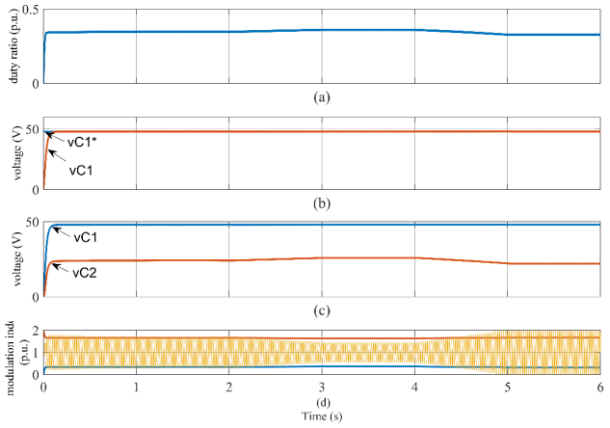

Figure 11. Simulation results for the single-phase qZSI model with PV array as input voltage source under varying irradiance and temperature (a) shoot-through duty ratio d_o, (b) reference v_{C1}^* and measured v_{C1} voltages across capacitor C_1, (c) voltages measured across capacitor C_1 and C_2, and (d) modulating waveform v_m

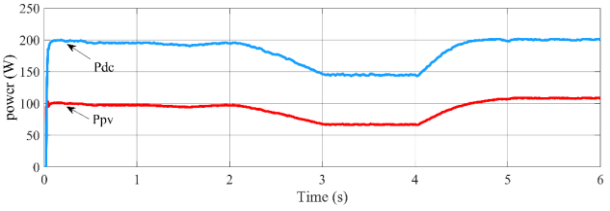

Figure 12. Simulation results of input power P_{PV} and output power P_{dc}

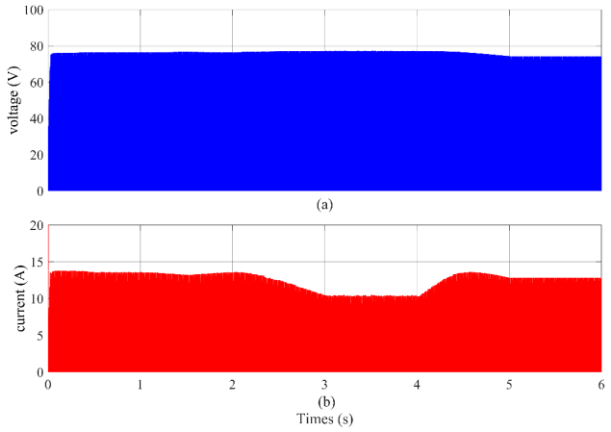

Figure 13. Simulation results of (a) DC-link voltage V_{DC} and (b) DC-link current I_{DC}

The zoomed in view of Figure 13 was shown in Figure 14 to verify the design of this work. Specifically, the operating mode of qZSI (e.g., either in continuous conduction mode, at boundary condition, or discontinuous conduction mode) is affected by the selection of switching frequency, size of inductor, and the size of load.

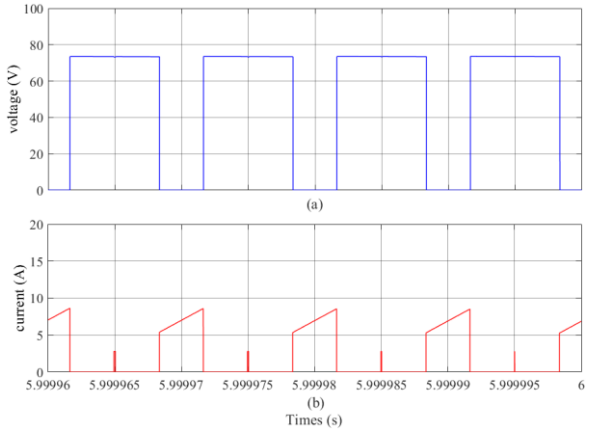

Figure 14: Zoomed in simulation results of (a) DC-link voltage V_{DC} and (b) DC-link current I_{DC}

The inversion of DC waveforms to AC waveforms through the single-phase H-bridge inverter is shown in Figure 15 with its zoomed in view illustrated in Figure 16.

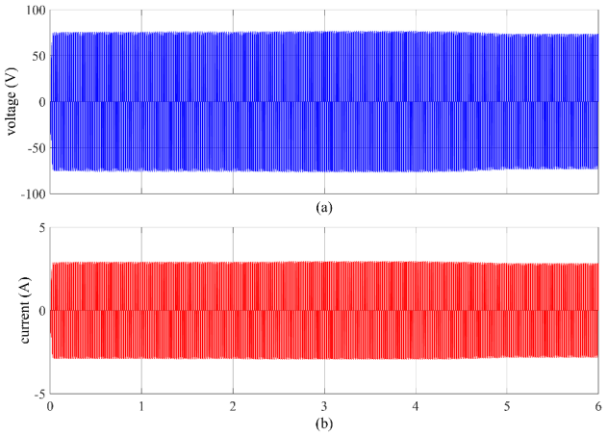

Figure 15. Simulation results of generated (a) AC voltage v_o and (b) AC current i_o

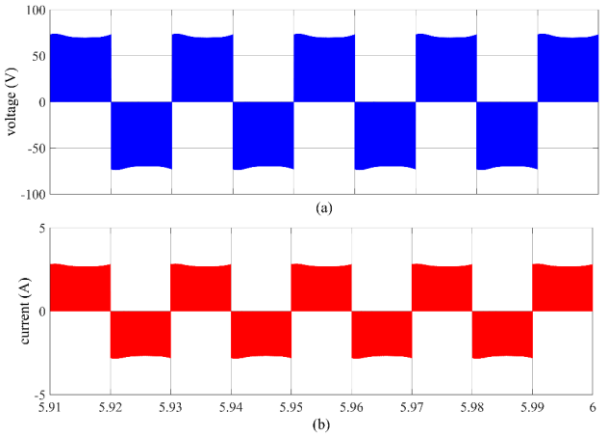

Figure 16. Zoomed in simulation results of (a) AC voltage v_o and (b) AC current i_o

The percentage of total harmonic distortion (THD) of AC output voltage v_o generated via the qZSI is shown at the frequency spectrum of Figure 17 below.

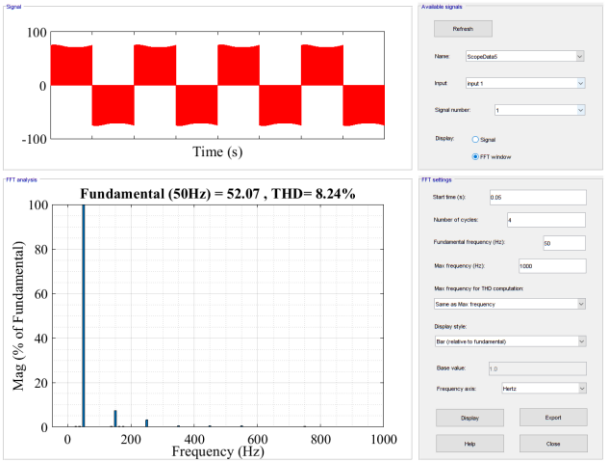

Figure 17. Frequency spectrum of AC voltage waveform v_o generated by the qZSI

According to the IEEE 519-2014, the THD generated from the proposed qZSI is on par with the standard.

Last but not least, all aforementioned proposed work are extended to grid application as STATCOM to improve its power factor. The grid parameters with power factor of 0.7 is tabulated in Table 2.

Table 2. System parameters for grid and load

Parameters	**Value**
Grid Voltage, v_s	12 V
Grid resistance, R_s	0.026 Ω
Grid inductance, L_s	0.82 mH
Coupling resistance, R_c	2.6 Ω
Coupling resistance, L_c	0.082 H
Load resistance, R_l	18.4 Ω
Load inductance, L_l	0.06 H

From Figure 18, it can be observed that the grid source voltage v_s and current i_s is almost in-phase (see Figure 18(a)) when compared with the load one (see Figure 18(c)) indicating the superiority of the proposed PV integrated Qzsi.

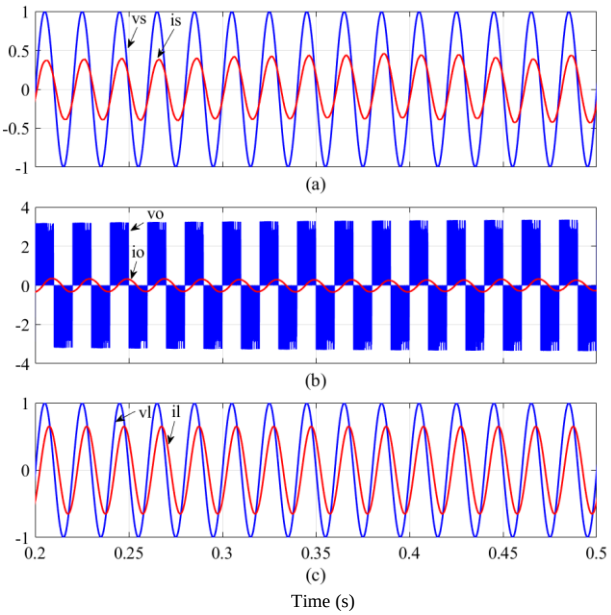

Figure 18. Simulation results of AC (a) grid voltage and current, (b) qZSI voltage and current, and (c) load voltage and current

V. CONCLUSION

The proposed dual-loop DC-link voltage controller and the grid-tie controllers were designed through detailed mathematical derivations and the feasibility of the controllers were verified through simulation via MATLAB/Simulink. With the application of the lead compensator, the proposed dual-loop DC-link voltage controller produced desired shoot-through duty ratio feeding to the CB-PWM modulator. On the other hand, the proposed grid-tie controller was able to produce desired modulating waveform to generate switching pulses for driving the qZSI. The P&O algorithm was applied as the MPPT technique for the proposed qZSI model to ensure maximum power extraction from the PV array. Subsequently, with the integration of the proposed controllers and the MPPT algorithm, the single-phase three-level qZSI model was able to ensure maximum power to be delivered to the load and also achieve constant DC-link voltage under constant and varying solar irradiance and temperature conditions.

VI. REFERENCES

Chung, T.M., Daniyal, H., Sulaiman, M. & Bakar, M. 2018, 'Comparative study of p&o and modified incremental conductance algorithm in solar maximum power point tracking', in *4th IET Clean Energy and Technology Conference*, 14 November 2016, Kuala Lumpur, Malaysia.

Cindy, P.Y.L., Law, K.H. & Lim, K.H. 2019, 'Direct Fast Charging of Electric Vehicle Using Solar Power', in *7th International Conference on Smart Computing & Communications*, 28 June 2019, Sarawak, Malaysia.

Gorgani, A., Elbuluk, M., Sozer, Y. and Rub, H.A. 2017, 'Quasi-z-source-based multilevel inverter for single phase pv applications', in *IEEE Energy Conversion Congress and Exposition*, 18 September 2016, Milwaukee, WI, USA.

Hanafiah, S., Ayad, A., Hehn, A. & Kennel, R. 2017, 'A hybrid mppt for quasi-z-source inverters in pv applications under partial shading condition', in *11th IEEE International Conference on Compatibility, Power Electronics and Power Engineering*, 4 April 2017, Cadiz, Spain.

Islam, M.N., Rahman, M.Z. & Mominuzzaman, S.M. 2014, 'The effect of irradiation on different parameters of monocrystalline photovoltaic solar cell', in *3rd International Conference on the Developments in Renewable Energy Technology*, 29 May 2014, Dhaka, Bangladesh.

Law, K.H. & Dahidah, M.S.A. 2014, 'DC-DC boost converter based MSHE-PWM cascaded multilevel inverter control for STATCOM systems', in *2014 International Power Electronics Conference*, 18 May 2014, Hiroshima, Japan.

Law, K.H. & Dahidah, M.S.A. 2014, 'New current control algorithm incorporating multilevel SHE-PWM approach for STATCOM operation under unbalanced condition', in *2014 IEEE 5th International Symposium on Power Electronics for Distributed Generation Systems*, 24 June 2014, Galway, Ireland.

Law, K.H. & Ng, W.P.Q. 2019, 'Dual closed-Loop scheme with lead compensator and proportional controller for quasi z-source inverter based STATCOM', in *2018 IEEE 7th International Conference Power and Energy*, 3 December 2018, Kuala Lumpur, Malaysia. 2019e

Law, K.H. 2019, 'Mathematics modelling and simulation of batteries charging capability in quasi Z source impedance network', in *7th International Conference on Smart Computing & Communications*, 28 June 2019, Sarawak, Malaysia. 2019.

Law, K.H., Dahidah, M. & Mariun, N. 2011, 'Cascaded multilevel inverter based statcom with power factor correction feature,' in *2011 IEEE Conference on Sustainable Utilization and Development in Engineering and Technology*, 20 October 2011, Semenyih, Malaysia.

Law, K.H., Dahidah, M., Sim, S.Y., Ng, W.P.Q., Masaoud, A. & Siada, A.A. 2019, 'An effective dual closed-loop scheme based on lead compensator and proportional controller for quasi z-source inverter', in *2018 IEEE Region 10 Conference*, 28 October 2018, Jeju, Korea. 2019d

Law, K.H., Dahidah, M.S.A., Konstantinou, G.S. & Agelidis, V.G. 2012, 'SHE-PWM cascaded multilevel converter with adjustable DC sources control for STATCOM applications', in *proceedings of the 7th International Power Electronics and Motion Control Conference*, 2 June 2012, Harbin, China.

Law, K.H., Loh, W.N. & Wong, K.I. 2019, 'Mathematics derivation and simulation modelling of maximum power

point tracking-based controller for quasi z source inverter', in *7th International Conference on Smart Computing & Communications*, 28 June 2019, Sarawak, Malaysia. 2019a

Law, K.H., Ng, W.P.Q. & Au, P.I. 2019, 'Design, Modelling and Control Implementation of PV-MPPT Based DC-DC Converter for STATCOM', *IOP Conference Series: Materials Science and Engineering*, vol. 495, iss. 1, pp. 012035. 2019b

Law, K.H., Ng, W.P.Q. & Wong, K.I. 2019, 'Active Harmonic Filtering Using Multilevel H-bridge Inverter Based STATCOM', *IOP Conference Series: Materials Science and Engineering*, vol. 495, iss. 1, pp. 012036. 2019c

Law, K.H., Ng, W.P.Q. & Wong, W.K. 2017, 'Flyback cascaded multilevel inverter based SHE-PWM control for STATCOM applications', *International Journal of Power Electronics and Drive Systems*, vol. 8, no. 1, pp. 100-108.

Meraj, S.T., Ahmed, A., Law, K.H., Arif, A. & Masaoud, A. 2019, 'DSP Based Implementation of SHE-PWM For Cross-Switched Multilevel Inverter', in *2019 IEEE 15th International Colloquium on Signal Processing and its Applications*, 8 March 2019, Penang, Malaysia.

Meraj, S.T., Law, K.H. & Masaoud, A. 2019, 'Simplified Sinusoidal Pulse Width Modulation of Cross-switched Multilevel Inverter', in *2019 IEEE 15th International Colloquium on Signal Processing and its Applications*, 8 March 2019, Penang, Malaysia.

Ong, J.S.X., Yong, K.S.K., Law, K.H., Ng, W.P.Q. & Dahidah, M. 2018, 'CCM and DCM analysis of quasi-z-source inverter', in *2017 IEEE Conference on Energy Conversion*, 30 October 2017, Kuala Lumpur, Malaysia.

Rehmani, M.H., Reisslein, M., Rachedi, A., Erol-Kantarci, M. & Radenkovic, M. 2018, 'Integrating renewable energy resources into the smart grid: Recent developments in information and communication technologies', *IEEE Transaction on Industrial Informatics*, vol. 14, no. 7, pp. 1551-3203.

Sia, Y.W. & Law, K.H. 2019, 'Deep analysis of quasi z source inverter for batteries charging and discharging capabilities across all DC capacitors' terminals', in *7th International Conference on Smart Computing & Communications*, 28 June 2019, Sarawak, Malaysia.

Skoplaki, E. & Palyvos, J. 2009, 'On the temperature dependence of photovoltaic module electrical performance: A review of efficiency/power correlations', *Solar energy*, vol. 83, no. 5, pp. 614-624.

Yong, S.K., Law, K.H., Ng W.P.Q. & Dahidah, M. 2018, 'Lead compensator design for single-phase quasi Z-source inverter', *Journal of Telecommunication, Electronic and Computer Engineering*, vol. 10, iss. 1-12, pp. 39-44.